



DD  
J. H. Dugay  
HE OUT

## LARGE AREA HORIZONTAL DRIFT CHAMBERS FOR A FOCAL PLANE POLARIMETER AT THE TRIUMF MEDIUM RESOLUTION SPECTROMETER\*

R.S. Henderson<sup>1</sup>), O. Haussler<sup>2</sup>), K. Hicks, C. Gunther<sup>3</sup>), W. Faszer

R. Sawafra<sup>4</sup>), and N. Poppe

TRIUMF, 4004 Wesbrook Mall, Vancouver, B.C., Canada V6T 2A3

- 1) also affiliated with University of Melbourne, Australia
- 2) also affiliated with Simon Fraser University, Canada
- 3) visitor from University of Bonn, West Germany
- 4) also with University of Alberta, Canada

### Abstract

Horizontal drift chambers of a relatively simple and inexpensive design are described. Four of these, each with an active area of  $0.89 \times 0.49 \text{ m}^2$ , constitute the basic detector system for a new focal-plane polarimeter at the medium resolution spectrometer (MRS) at TRIUMF. The inherent left-right ambiguity in the direction of drift was resolved using the  $\sim 15\%$  difference in the signals induced on adjacent (odd or even) cathode wires. With separate charge integration of the pulses, a normalized and corrected odd-even difference is obtained from which the horizontal drift direction is reliably deduced. The odd-even difference is found to depend sensitively on the accuracy with which the anode wire is centered in the unit cell.

(Submitted to Nuclear Instruments and Methods)

\*Supported in part by Natural Sciences and Engineering Research Council of Canada

### When the decision was taken at TRIUMF to construct a polarimeter encompassing the full length of the MRS focal plane, the detectors were specified to have an active area of $\sim 0.5 \text{ m}^2$ . Position resolution of better than 1 mm in both X and Y directions, perpendicular to the incident charged particles, was a further requirement. A delay-line readout design was chosen based on the detector system for the EPICS spectrometer at LAMPF[1]. Delay-line determination of the avalanche anode wire position has the advantage of low electronic readout cost since only two timing channels are required independent of the number of anode wires in a chamber plane. The wire plane consists of alternating anode and cathode wires, corresponding to a cell size of 8.13 mm (maximum drift distance of 4 mm). With a careful choice of electronic components (low-noise preamplifiers and constant-fraction discriminators) we obtain wire spectra from the time differences which are highly linear and nearly independent of pulse height. Drift time information can also be obtained by summing the times from each end of the delay-line with respect to a prompt timing signal derived from a fast scintillator.

The drift time mentioned above could be used for position interpolation between anode wires, were it not for the left-right ambiguity, i.e. two tracks located at the same distance from, but on either side of, the anode wire cannot be distinguished. This ambiguity is however requires doubling the number of wire planes and also has a parallax problem which can lead to incorrect left-right assignments unless position information from several chambers is used to test for a straight-line trajectory.

In this paper a method is described which continues and improves on earlier work on the left-right problem [2,3]. We use the small (~15%) difference in the signals induced on adjacent cathode sense wires. Alternate cathode signals are bussed out on ODD and EVEN outputs. Rather than using matched analogue subtraction circuits to obtain O-E [3], we amplify and encode the ODD and EVEN signals separately and calculate a normalized and corrected difference,  $(O-E \cdot C_w) / (O+E \cdot C_w)$ , where  $C_w$  is a correction factor for a specific wire. With this technique we obtain a reliable solution to the left-right ambiguity for minimum ionizing particles.

## 2. Chamber Construction

Each of the four chambers consists of two orthogonal wire planes, three cathode foils and two gas window foils. These seven planes are each 4.8 mm apart. Two 12.7 mm tooling plates are used to maintain the flatness of the stack. O-ring seals between each layer provide a gas seal. The cathode planes consist of vacuum-stretched, 25  $\mu\text{m}$  thick, doubly-aluminized mylar, epoxied to 4.8 mm thick aluminum plates. These cathode foils are held at ground potential.

A schematic view of one of the orthogonal wire planes is shown in Fig. 1. The wire planes consist of alternating anode and cathode wires, with an anode-cathode spacing of 0.160 inch (~4 mm). The anode wires are of 20  $\mu\text{m}$  gold-plated tungsten tensioned to 45 g. At one end these are soldered directly to a low loss delay-line [1]. The anode wires and delay line are held at a positive high voltage. The cathode wires are of 75  $\mu\text{m}$  gold-plated beryllium-copper and tensioned to 95 g. They are alternately bussed together to form two cathode outputs, ODD and EVEN, for each wire plane.

The drift cell configuration of the detector is shown in the lower part of Fig. 1. A novel feature of the TRIUMF detectors is the use of a pair of cathode wires 0.5 mm apart. The electric fields for this and the conventional configuration are compared in Fig. 2. Near the cathode wires the field strength is enhanced and the induced cathode signals are observed to be larger by 40 to 50%. This improvement is significant in view of the fact that the left-right separation was found to deteriorate at higher operating voltages, in spite of larger induced signals (see discussion below). The chambers constructed for the TRIUMF polarimeter have active areas 89 cm  $\times$  49 cm and consist of 110 and 60 active anode wires in the X and Y directions, respectively.

## 3. Electronics, signal encoding and processing

The electronic arrangement for one wire plane is shown schematically in Fig. 3. The timing electronics for the delay lines consists of commercially available elements which were selected to ensure optimum performance. The signals from each end of the delay line were amplified in fast amplifiers (EGG VT110A) which combine high gain ( $\times 150$ ), large bandwidth (1 GHz), and low input noise (<40  $\mu\text{V}_{\text{pp}}$ ). Timing signals were derived from the amplified pulses using constant fraction discriminators (Tennelec TC454), the external cable delays being optimized to 13 ns for X-planes and 15 ns for Y-planes. Pulses from the 1 m long delay line exhibit a considerable variation in risetime and amplitude, depending on whether the event originated at the near or far end. Since a single CFD delay cannot be near optimum for a large variation in risetime, we have introduced a small series inductance ( $L=L_{\text{sh}}H$ ) at each end of the delay line. With the preamp input resistance of 50 ohms this low-pass LR circuit degrades both the risetime and amplitude of the fastest pulses to

more closely approximate those of the slower pulses. Using minimum ionizing electrons from a  $^{106}\text{Ru}$  source, we obtained trigger efficiencies per wire plane in excess of 0.99.

The bussing-together of many (60 or 110) cathode wires to common ODD or EVEN outputs implies large capacitances and significant dispersion of the cathode signals. The pulse propagation time along the readout direction is 20 ns/m for both X and Y planes. Fast two-stage amplifiers were designed and built at TRIUMF to boost the ODD and EVEN signals. Typical pulses have slow risetimes (~25 ns) and decay times (~150 ns). The amplified ODD and EVEN pulses are input to charge-sensitive ADC's (LeCroy 2249SG) with 50 ns wide gate pulses. Separate gates are necessary for each wire plane because of the jitter in the drift times (0-80 ns) relative to the prompt pulses from the trigger scintillators.

For each detector plane we encode three timing signals:  $T_1$  and  $T_r$ , the TDC times for each end of the delay line, and  $T_c$ , the cathode timing signal. Also encoded are the ADC amplitudes of the two cathode signals, Odd and Even. From these we generate:

- 1) The anode wire position,  $T_1 - T_r$
- 2) The drift time  $T_d$  from the anode timing,  $T_1 + T_r - 2T_d + \text{const}$
- 3) The drift time ' $T_d'$ ' from the cathode timing, corrected for the propagation time along the readout direction,  $T_d' = T_c - (T_1 - T_r) * f$
- 4) A CHECKSUM spectrum,  $T_1 + T_r - 2T_d' = (2T_d - 2T_d') + \text{const}$
- 5) A normalized cathode difference spectrum,  $(E_{\text{odd}} - E_{\text{even}}) / (E_{\text{odd}} + E_{\text{even}})$ .

The CHECKSUM spectrum contains a sharp peak from 'good' events and is used for rejection of multiple events in a wire plane. Two nearly coincident avalanches in a wire plane can cause the  $T_1$  and  $T_r$  stop signals to come from different avalanches. This can look like a single

event in a third position but appears outside the peak in the CHECKSUM spectrum. Several two-dimensional combinations of the above parameters have proved to be of value in understanding the chamber characteristics (see the following section).

#### 4. Results

The chamber performance was evaluated using protons from the  $^{12}\text{C}(\text{p},\text{p}')$  reaction at  $E_p=400$  MeV. The chambers were in their final location above the MRS focal plane and the magnetic field of the MRS dipole was set to illuminate the focal-plane (X direction) with a continuous proton distribution.

##### 4.1. Delay-line readout

A histogram of delay line time differences is shown in Fig. 4. The wires are seen to be well separated, including the edge regions. A fit of the peak centroid positions versus wire number results in a very small quadratic term, with deviations from linear fits amounting to <0.3 wire separations over the 110 wires. The sum of the delay line times,  $T_1 + T_r$ , shown in Fig. 5, was used to obtain a drift time-to-distance calibration.

Following the procedure described by Breskin et al.[4] an evenly illuminated drift cell produces a drift time distribution  $dN/dt$  which is related to the spatial distribution of particles,  $dN/ds=\text{const}$ , by

$$dN/dt = (dN/ds) * (ds/dt) = \text{const} * v(t) \quad (1)$$

where  $v(t)$  is the drift velocity. Then the avalanche position

$$s(t) = (1/c) * \int_0^t (dN/dt) dt \quad (2)$$

is obtained from a lookup table containing the normalized interpolation integral (2) for the range of drift times  $T_d$ . Because of the excellent

timing properties of the delay lines the drift time spectrum  $T_d$  is of better quality than the spectrum  $T_d'$  derived from the cathode timing.

#### 4.2. Left-right ambiguity

A reliable determination of the direction of drift from the induced cathode signal amplitudes turned out to be not completely straightforward. Tests both with betas from  $10^6$  Ru and with 400 MeV protons showed that the strength of the induced signal varies strongly, becoming smaller near the anode or the cathode. This is apparent from Fig. 6 where the average induced pulse heights corrected for ADC offsets,  $(O+E)/2$ , are shown versus drift time. Because of the large variation in  $(O+E)$  it is more appropriate to use the normalized difference,  $D=(O-E)/(O+E)$ , rather than  $(O-E)$  as the discriminator for the direction of drift. On some sections of the chambers, e.g. the one shown in Fig. 7, the asymmetry  $D$  exhibits a pronounced 'staggering' effect when plotted versus anode wire position (top half of Fig. 7). Since 'left' cathode wires are bussed alternately on to ODD or EVEN outputs depending on whether the wire number is an odd or even integer the staggering could arise from a systematic displacement of the anode wire from the centre of the unit cell towards one side. This interpretation has been proven conclusively by scanning the same wire plane under a travelling microscope. The correlation between the wire-positioning error and the location of the minima between the two peaks of the asymmetry  $D$  (which is normalized to "b" the separation of the peaks) is shown in Fig. 8. We point out that an anode centering error of  $50 \mu\text{m}$  or  $0.6\%$  causes the minimum to shift by as much as 25%. To avoid the need for software corrections, a wire centering accuracy of less than plus or minus  $7 \mu\text{m}$  would be required. Such tolerances are very difficult to maintain in

wires 1 m long, due to electrostatic instabilities. This sensitivity to wire position accuracies was probably not realized previously and may account for the fact that this technique of using the differences in the induced cathode signals has not been widely adopted.

Once the origin of the 'staggering' in Fig. 7 was understood an improved asymmetry,  $D'=(O-E*C_w)/(O+E*C_w)$ , was constructed with  $C_w$  being a factor for each wire which is stored as a constant in the computer. The factors  $C_w$  are easily determined by obtaining the centroid of the  $(O-E)/(O+E)$  distribution, for each wire. With even illumination of the cell this corresponds to the location of the minimum in the distribution, which ideally should be at zero. A simple formula relates the centroid of this distribution ( $E_c$ ) to the correction value  $C_w$ , given by

$$C_w = (1+E_c)/(1-E_c). \quad (3)$$

The correction factors  $C_w$  have proven to be a stable property of the chambers. The new asymmetry  $D'$  shows a clear separation between the two directions of drift (see Fig. 7, lower half).

These correction factors  $C_w$  applied to the ODD pulse heights make it unnecessary to distinguish further between different wires. The two-dimensional figures 9 and 10 are obtained using information from 110 X-wires. Fig. 9 shows  $E_{odd}$  versus  $E_{even}$ , with two clearly separated bands associated with the two drift directions. From Fig. 10 which shows  $D'$  versus the drift time, it is seen that the direction of drift cannot be determined in the immediate vicinity of the anode. Apparently the drift electrons do not approach the anode wire from the plane of the wires, causing a degradation in the asymmetry. Fortunately, the resulting ambiguity is of little consequence since the drift correction is very small for events near the anode. The overall position resolution of

the chambers has been measured with protons of several energies between 250 and 400 MeV. With three chambers spaced 20 cm apart a single plane resolution of 0.3 mm FWHM was determined from the residuals of straight line fits to the trajectory [see ref. 5].

#### 8. Operation and conclusions

The chambers described here are operated with a gas mixture of 65% argon, 35% isobutane, and 0.50% isopropyl alcohol at 760 Torr and a voltage of 2050 V. We have found that addition of freon in the mixture, even at the 0.10% level, degrades markedly the efficiency of long drift time events and should be avoided. The chambers have been used in the MRS focal plane polarimeter and have operated extremely reliably in a number of experiments [see Ref. 5]. Although chamber rates of 500 KHz have been used without problems, the polarimeter dead times (with eight wire planes) are high because of the long readout time for the delay lines (235 ns). For this reason DC rates of 100-150 KHz have been more common.

Above 2250V a new gas gain mode begins to develop. This onset of the limited streamer mode is accompanied by bigger signals, however the cathode difference signal fails increasingly as a discriminator for the direction of drift. It appears likely that avalanches begin to spread around the anode wire. The construction with pairs of cathode wires, while more elaborate, improves significantly the field configuration near the cathode wires and leads to a valuable increase in the cathode signal amplitudes.

The calculation of a normalized and corrected asymmetry  $(O-E*C_w)/(O+E*C_w)$  has proven a reliable solution to the left-right ambiguity.

#### References

- [1] C.L. Morris, H. A. Thiessen and G. W. Hoffman, IEEE Trans. of Nuclear Science Vol. NS-25, No.1 (1978) 141.
- [2] A.H. Walenta, Nucl. Instr. and Meth. 151 (1978) 461.
- [3] L.G. Atencio, J. F. Amann, R. L. Boudrie and C. L. Morris, Nucl. Instr. and Meth. 187 (1981) 381.
- [4] A. Breskin, G. Charpak, G. Gabiou, F. Sauli, N. Trautner, W. Duinker and G. Shultz, Nucl. Instr. and Meth. 119 (1974) 9.
- [5] O. Haussler, R. Henderson, K. Hicks, D. Hutcheon, D. Clark, C. Gunther, R. Sawafta, and G. Waters, following paper.

**Figure Captions**

1. Schematic view of one of the wire planes showing the alternating anode-wire cathode-wire geometry. The cathode wires are in pairs 0.5 mm apart.
  2. Field calculation for single-cathode and double-cathode wire geometry. Showing improved track collection near the cathodes with the added wire.
  3. Electronic readout arrangement for one wire plane.
  4. The delay-line time difference ( $T_1-T_R$ ) distribution is plotted. It shows the anode wires are well resolved including those at the very edges, 110 wires in this case.
  5. The drift time distribution, with the value of drift time ( $T_d$ ) calculated from the delay line timing ( $T_1+T_R=2T_d+t_{const}$ ).
  6. The average induced pulse height on the cathode buses vs drift time, showing the signals become smaller near the anode (short drift) and the cathodes (long drift).
  7. Asymmetry ( $E-0)/(E+0)$  and corrected asymmetry  $(E-0*C_w)/(E+0*C_w)$  vs delay line time differences ( $T_1-T_R$ ). Each group in time difference corresponds to one anode wire. The  $C_w$  values represent a correction factor for each wire to compensate for small wire centering errors.
  8. The wire position error and the location of the minima in the  $O-E$  distribution (normalized to separation of the maxima) vs wire number. The strong correlation indicates that the difference signal is very sensitive to small wire positioning errors.
9. The pulse height distribution of "odd" vs "even" cathode signals for the plane after  $C_w$  corrections. The two bands correspond to the two directions of drift.
  10. The corrected odd-even asymmetry vs drift time. The two directions of drift are clearly separated, except for tracks passing very close to the anode wire.

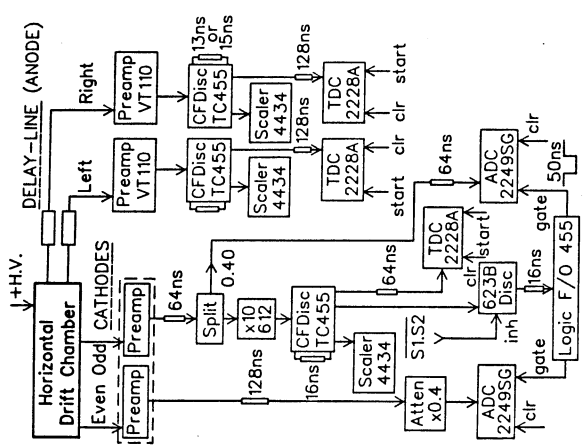


Fig. 3

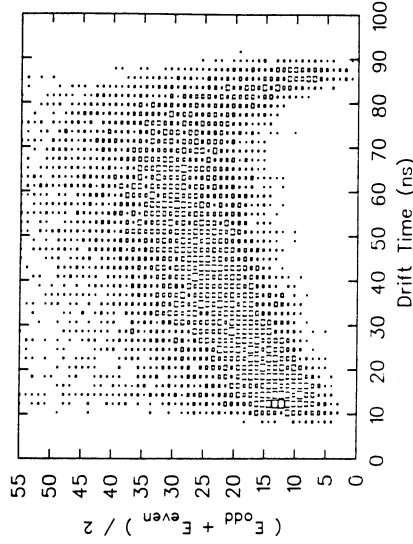


Fig. 6

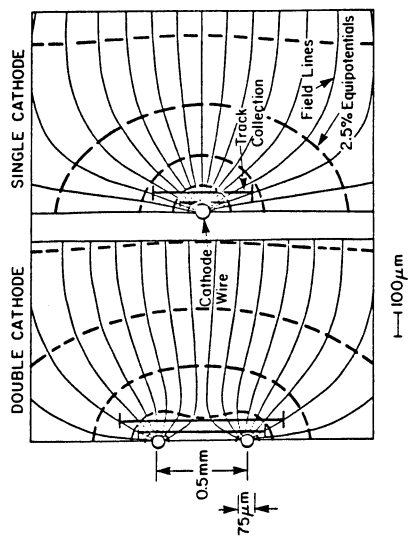


Fig. 2

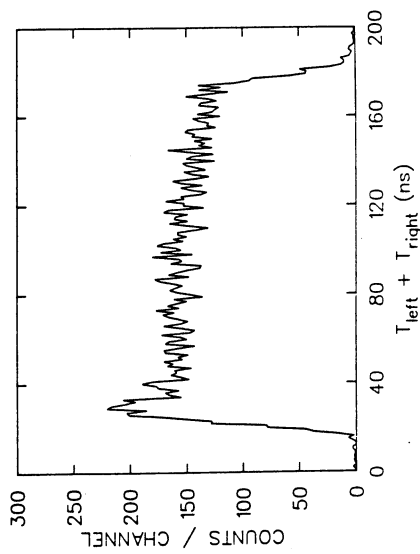


Fig. 5

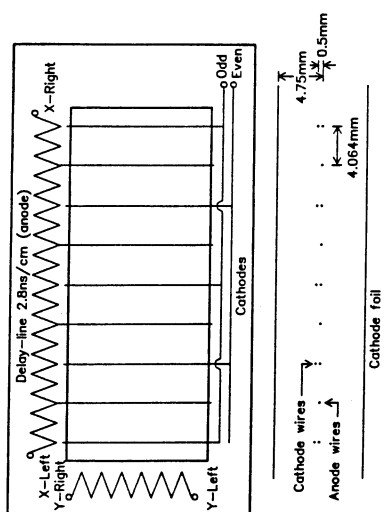


Fig. 1

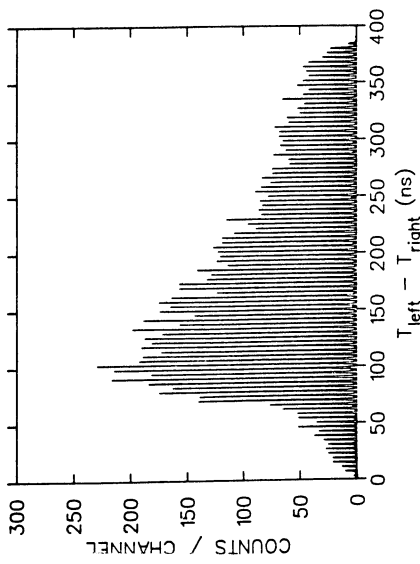


Fig. 4

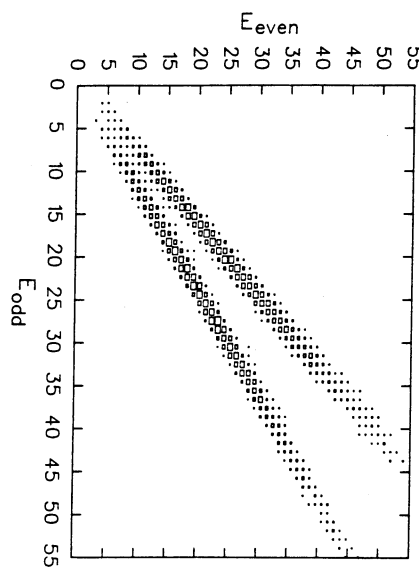


Fig. 9

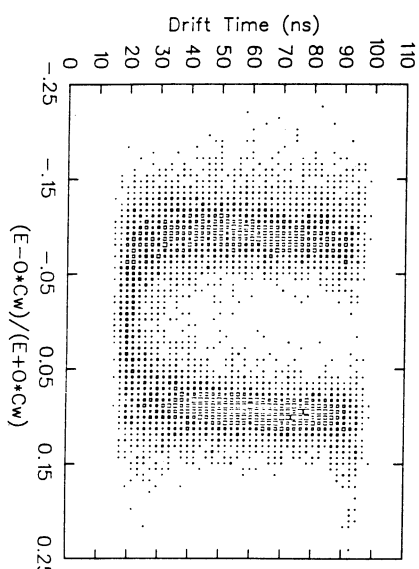


Fig. 10

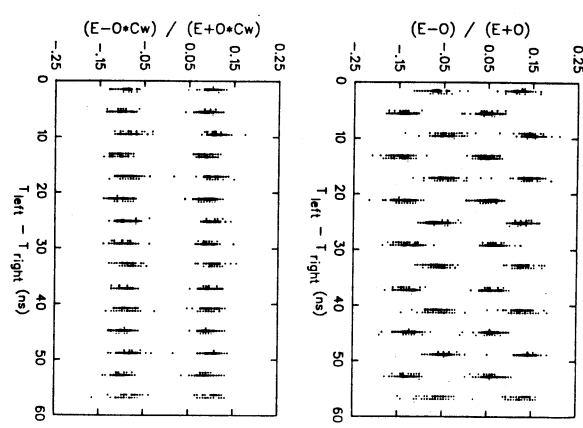


Fig. 7

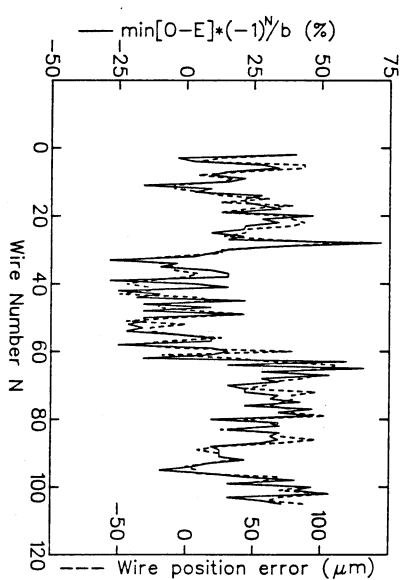


Fig. 8